Article, Published Version

Becker, Marius; Maushake, Christian; Winter, Christian

Mud-induced periodic stratification in a hyper-turbid estuary

Geophysical Research Letters

AGU100 ADVANCING EARTH AND SPACE SCIENCE

Geophysical Research Letters

RESEARCH LETTER
10.1029/2018GL077966

Key Points:
- Forced by an asymmetric tide, the flow structure in a hyperturbid tidal channel is controlled by mud-induced periodic stratification
- Restratification during flood leads to vertical decoupling, counterdirected flow, and the development of an inverse salinity profile
- Intratidal transport of mud depends on the entrainment asymmetry, inducing upstream pumping during flood and shear dispersion during ebb

Correspondence to:
M. Becker,
mbecker@marum.de

Citation:
Becker, M., Maushake, C., & Winter, C. (2018). Observations of mud-induced periodic stratification in a hyperturbid estuary. *Geophysical Research Letters*, *45*, 5461–5469. https://doi.org/10.1029/2018GL077966

Received 20 MAR 2018
Accepted 28 APR 2018
Accepted article online 9 MAY 2018
Published online 5 JUN 2018

Observations of Mud-Induced Periodic Stratification in a Hyperturbid Estuary

Marius Becker[1], **Christian Maushake**[2], **and Christian Winter**[1]

[1]MARUM - Center for Marine Environmental Sciences, University of Bremen, Bremen, Germany, [2]BAW - Federal Waterways Engineering and Research Institute, Hamburg, Germany

Abstract This study presents new observations of fluid mud transport and of the interaction between mud-induced stratification and the flow. Data collected in a hyperturbid estuarine tidal channel reveal details of the intratidal entrainment asymmetry, characterized by quasi-instantaneous entrainment and upstream pumping of mud during flood, and a gradual reduction of layer thickness by shear dispersion during ebb. Rapid restratification early during the flood phase restores the predominant two-layer structure and delimits the transport period, which is then significantly shorter than the overall flood duration. The hydraulic cross section is reduced, causing an increase of the salinity intrusion into the estuary at the end of the flood. The fluid mud layer occupies on average 40% of the water depth, and stratification exceeds that of highly stratified salt wedge estuaries. These data show how mud-induced periodic stratification influences flow structure and sediment transport and thereby contribute to the understanding of the dynamics of hyperturbid estuaries.

Plain Language Summary Deepening of navigational channels often leads to an increase of turbidity in estuaries. This increase may be extreme, with negative side effects for the environment, which are intensively discussed at present. While mud accumulates, it does not consolidate but is periodically mixed by tidal currents. This stage, called fluid mud, in turn changes the flow, in particular the vertical profile of flow velocities. This feedback is known in theory, but little information has been collected in the field. Long-term transport of mud in turbid estuaries is analyzed using models, but it is unclear if model results reflect the actual situation in nature. Due to the described effect of mud on the flow, detailed measurements are required, such as they are presented in this study. These data reveal several effects of mud on the flow, which have not been shown in sufficient detail before. An important aspect is the strong difference in mixing of mud between the ebb and the flood phase, which leads to a corresponding difference in mud transport. Any long-term change, in import or export of mud, depends on this balance. Therefore, results presented in this study significantly contribute to the understanding of mud transport in turbid estuaries.

1. Introduction

Environmental degradation and siltation pose great challenges to the management of estuaries, particularly in hyperturbid systems, where the increase in turbidity results from anthropogenic morphological changes (e.g., De Jonge et al., 2014). Then, deepening of the main channel, reduced friction, increased convergence, and the loss of intratidal area are considered to trigger changes in the tidal regime, increasing the trapping efficiency and accumulation of sediments (Van Maren et al., 2015; Winterwerp & Wang, 2013). Particularly in case of stagnating high-concentration layers, sediment-induced stratification can lead to hypoxic conditions, with severe consequences to the local ecosystem (De Jonge et al., 2014; Talke et al., 2011).

In hyperturbid estuaries, concentrations of suspended sediments (SSC) are on average far in the hindered settling regime. In the Ems estuary, tidal pumping causes the turbidity zone to be located upstream of the classical estuarine region, that is, the region of highest salinity gradients (Chernetsky et al., 2010). Fluid mud may cover the bed over several tens of kilometers along the channel, in the Ems estuary (Talke et al., 2009), or in the Humber-Ouse estuary (Uncles et al., 2006). Sediment concentrations in this layer introduce a significant density anomaly (Geyer et al., 2004; Kineke et al., 1996), such that the baroclinically influenced (estuarine) domain extends far upstream of the actual salinity intrusion. Along-channel (horizontal) pressure gradients are thus induced by both salt and suspended sediments, affecting the residual flow and the location of the turbidity zone (Donker & Swart, 2013; Talke et al., 2009).

Vertical sediment-induced stratification in hyperturbid estuaries is controlled by a balance of hindered settling and entrainment of fluid mud (Winterwerp, 2002; Wolanski et al., 1988). Periodic entrainment by tidal currents inhibits consolidation. SSC in the fluid mud layer is therefore below the gelling concentration, and the layer remains mobile, while its thickness may reach a significant fraction of the water depth (Kirby & Parker, 1983). Earlier measurements indicate the water column to exhibit a two-layer structure (Talke et al., 2009; Uncles et al., 2006), but its impact on flow structure and sediment transport was not analyzed in detail.

Fluid mud entrainment depends on tidal velocities. Model simulations of the flood-dominant tidal regime of the Ems estuary show that entrainment is increased during flood and that stratification persists during ebb (Winterwerp, 2011). Reduced flood velocities during high river discharge are suggested to cause a situation in which no entrainment occurs during flood (Winterwerp et al., 2017). In this scenario, high discharge conditions lead to fluid mud consolidation, instead of downstream mud transport and dispersion, which highlights the importance of intratidal processes, for example, of the entrainment asymmetry, for mud transport also on longer time scales.

While a significant number of model studies analyze processes that are relevant to hyperturbid estuaries (e.g., Dijkstra et al., 2018; Winterwerp, 2011), data on the actual situation in the field is practically unavailable in sufficient resolution, due to technical challenges regarding measurements in fluid mud (Sottolichio et al., 2011). This study provides new information on flow structure and sediment transport in hyperturbid conditions. Focusing on the distribution of turbulence, in situ data collected in the prototypically hyperturbid Ems estuary reveal details of the entrainment asymmetry, refining previous assumptions of fluid mud transport (Winterwerp et al., 2017), and show that the stabilizing effect of sediment-induced stratification is significantly more pronounced than generally considered.

2. Study Area and Methods

Data were collected in the Ems estuary at *Jemgum* (Figure 1a). Further downstream, in the lowest part of the tidal river ($>$ km 30), the transport regime is always flood dominant (Winterwerp et al., 2017). Fluid mud covers a stretch of up to 30 km in the tidal river (Figure 1e), on average located between river km 0 and 30 (Talke et al., 2009).

During the measurements, the ship was moored at the navigation channel. A sediment echo sounder (SES) and an acoustic Doppler current profiler (ADCP; 600 kHz) were deployed on a floating platform next to the ship. At the same station, velocities were also measured by two electromagnetic current meters (ECM), each deployed at a fixed height above the consolidated river bed (indicated in Figure 2a).

Near-bed velocities were filtered to remove bias by spikes, which occurred in ADCP data due to high SSC near the bed (Cao et al., 2012). An 8-min moving average filter was applied to the cleaned ADCP velocity profile and to each ECM velocity time series. The inductive velocity measuring technique (by ECMs) is considered to be unbiased by high SSC. A comparison of the two independent techniques (upper ECM and ADCP) confirmed the validity of processed ADCP velocities data, which is subsequently used in the analysis.

Vertical conductivity-temperature-depth and optical backscatter sensor casts were collected every 0.5 hr, for a duration of 19.5 hr. The optical backscatter sensor was calibrated with respect to SSC obtained from filtered water samples. Vertical SSC profiles were interpolated in time along isolutals (Figure 2b). Salinity and SSC were taken into account calculating density, the buoyancy frequency $N^2 = -g\ \rho_0^{-1}\ \delta_z\rho$, the gradient Richardson number $Ri_g = N^2\ (\delta_z u)^{-2}$ (Richardson, 1920), and also the two-layer Froude number $G^2 = F_u^2 + F_l^2$, where the upper and lower layer Froude numbers F_u and F_l are based on layer-averaged values for velocity and reduced gravity (Armi & Farmer, 1986).

3. Mud-Induced Periodic Stratification

The density structure at the study site is characterized by stratification, mainly controlled by SSC (up to approximately 50 g/L). Subsequently, the term *mud-induced stratification* is used to acknowledge the effect

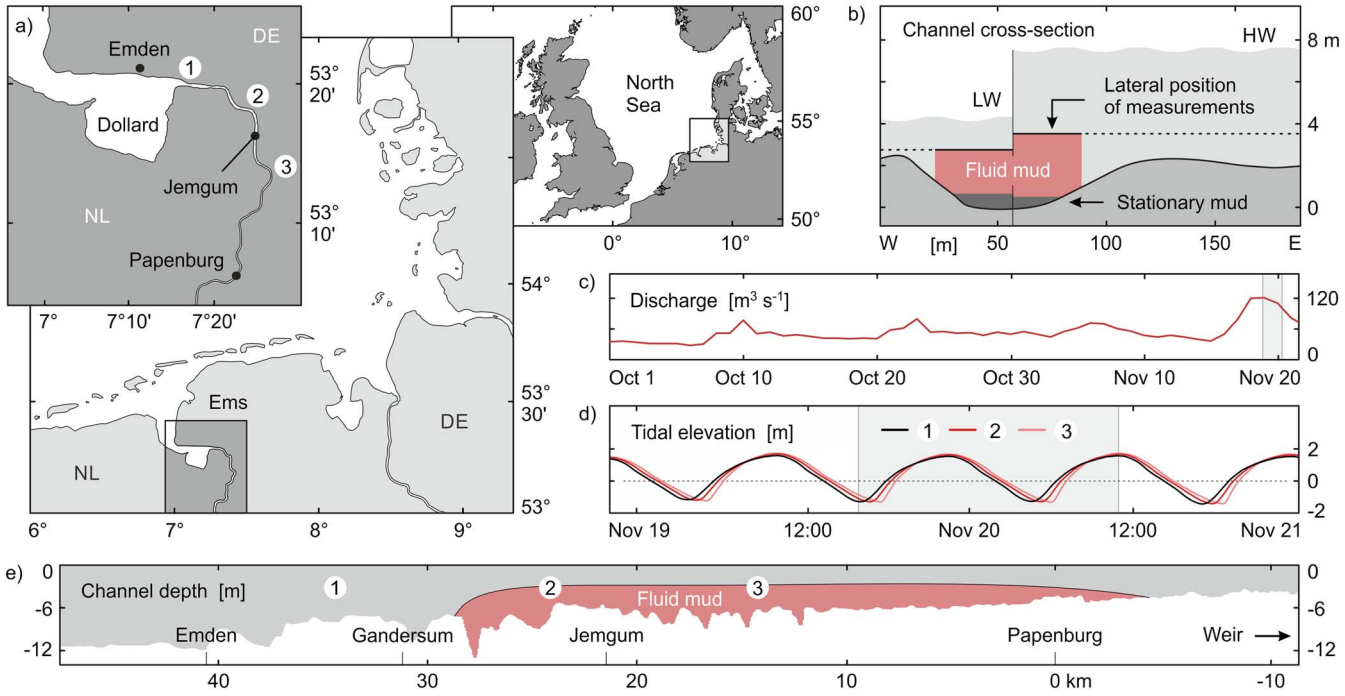

Figure 1. Study area and conditions during the measurements. (a) Location of the Ems tidal channel in the German Bight, North Sea. (b) Channel cross section. Stratification is depicted during high (HW) and low water (LW), as measured (see also Figure 2). (c) Discharge. (d) Tidal elevation at three gauges. Encircled numbers in (a) and (e) refer to their along-channel locations. Boxes in (c) and (d) indicate the measuring period, in 2014. (e) Along-channel depth profile, showing the approximate location of fluid mud.

of hindered settling (Dijkstra et al., 2018), promoting the formation of distinct interfaces in the vertical SSC profile, that is, local maxima in the vertical SSC gradient (δ_zSSC, Figure 2b).

A local maximum of δ_zSSC near the bed indicates the surface of stationary, consolidating mud. A transient second local δ_zSSC maximum, the lutocline (Kirby & Parker, 1983), separates the lower concentrated upper water column from high SSC near the bed. This region is referred to as *fluid mud layer*, irrespective of the state of mixing, that is, whether parts of the layer are turbulent or not.

3.1. Variations in Stratification

The tidal cycle is divided into five stages, differentiated by their characteristics of stratification (Figure 2). At the beginning of the flood (stage I), the fluid mud layer is entrained into the upper layer (Figure 2b). Upstream directed transport of sediments increases and reaches its maximum during the tidal cycle (Figure 2d). The stretching of isolutals indicates vertical mixing (Figure 2c), which results in a smooth vertical SSC profile, without distinct δ_zSSC maxima (Figure 2b, end of stage I). The buoyancy frequency is comparatively low ($N = 0.22\ s^{-1}$, Figure 2d).

The beginning of stage II is characterized by decreasing (flood) velocities and decreasing sediment transport. During stage II, settling increases and isolutals merge toward the vertical location (~ 3 m above the bed) of the lutocline during high water. The actual restratification (reformation of the fluid mud layer) is fast and occurs in less than 0.5 hr, indicated by a steep interface, which rises from the bed (marked in the SES profile, Figure 2c, end of stage II). Stage III comprises late flood, high water, and early ebb and is characterized by fully stratified conditions ($N_{max} = 0.7\ s^{-1}$), low current velocities in both layers, and negligible sediment transport.

During stage IV, ebb-directed sediment transport increases. In contrast to the mixing period during flood (stage I), near-bed SSC remains high (> 40 g/L). Stratification in the upper water column is almost constant ($N \cong 0.4\ s^{-1}$) and high in comparison to stage I (flood entrainment). This stratification persists until the following slack water. After a short settling phase during ebb slack water (< 2 m, stage V), the fluid mud layer thickness is reduced, compared to the end of the flood slack water (~ 3 m, stage III).

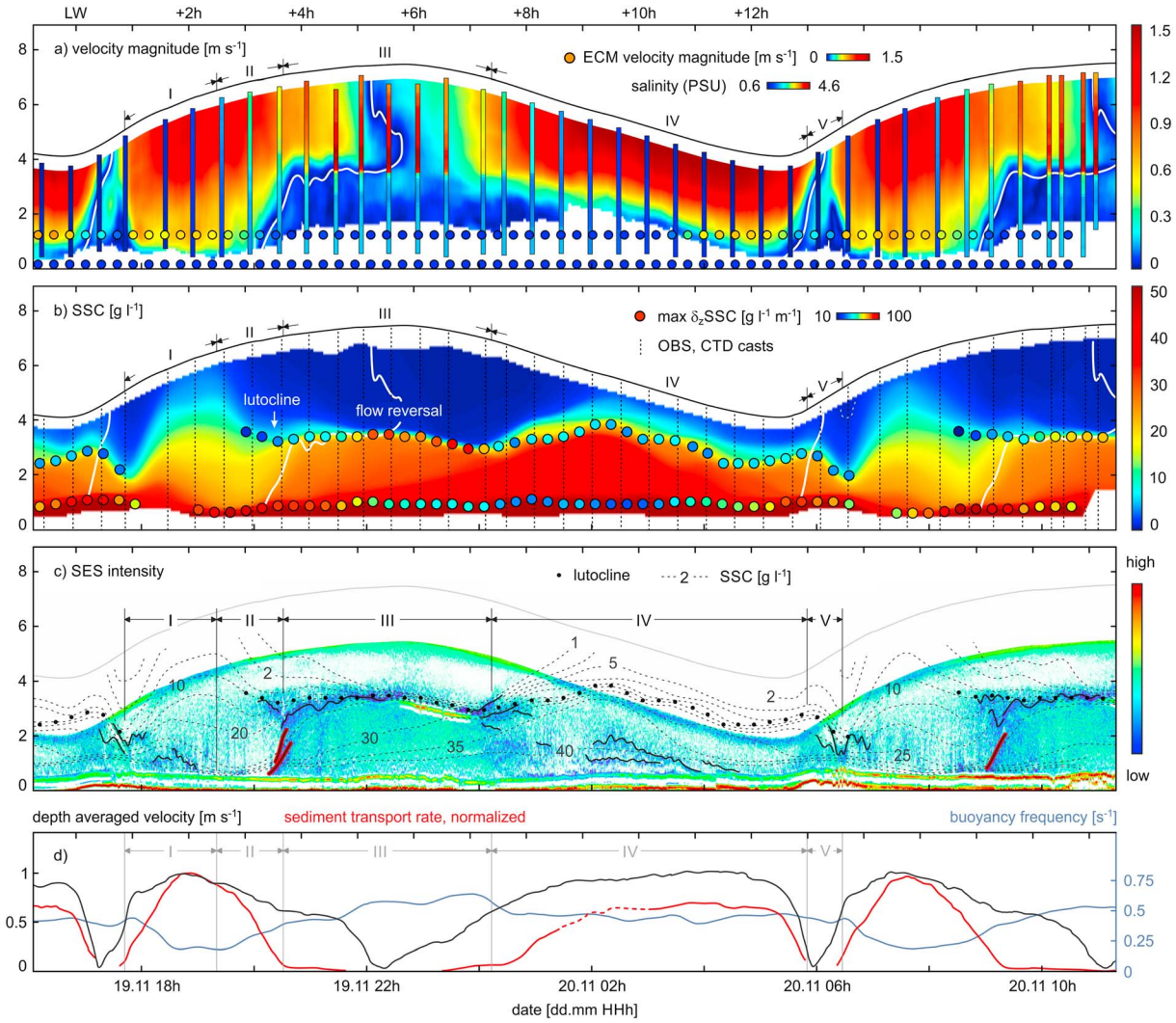

Figure 2. Velocity and stratification. (a) Velocity magnitude; vertical bars = salinity; colored circles = ECM velocity. (b) SSC; colored circles = local maxima of δ_zSSC (lutocline). (c) SES intensity; restratification is highlighted in red. (d) Depth-averaged velocity (black); vertically integrated sediment transport rate, normalized by maximum value (red); buoyancy frequency N (blue), calculated at the lutocline or at the 10 g/L isolutal, if a local δ_zSSC maximum does not exist. ECM = electromagnetic current meter; SSC = concentration of suspended sediments; SES = sediment echo sounder.

3.2. Entrainment Asymmetry

Entrainment of fluid mud is observed to be substantially different between flood and ebb. At the beginning of flood (stage I), flow acceleration is almost constant over the vertical, such that high velocities immediately reach down to the bed (Figure 3a, stage I). The fluid mud layer, as it exists after the ebb slack water, is *initially* advected in upstream direction. Peak values of mean velocity shear occur in a shallow region between the fluid mud layer and the bed (Figure 3b). There Ri_g drops below 0.25 (Figure 3c), which indicates a favorable situation for turbulence production (e.g., Trowbridge & Kineke, 1994). This triggers quasi-instantaneous entrainment of fluid mud and efficient mixing of sediment into the upper water column (see Bruens et al., 2012).

During early ebb, by contrast, flow acceleration is confined to the upper water column (Figure 3a, beginning of stage IV) and low in comparison to the flood (beginning of stage I). Shear increases above the lutocline, and Ri_g drops below 0.25 (Figure 3c). With decreasing tidal elevation, the region of high shear and low Ri_g propagates downward. Consequently, entrainment is a gradual process and occurs only at the layer surface (Figure 2c). The maximum depth of fluid mud entrainment is indicated by stratification observed in the SES profile at an almost constant water depth of approximately 4 m (Figure 2c). This is substantiated by

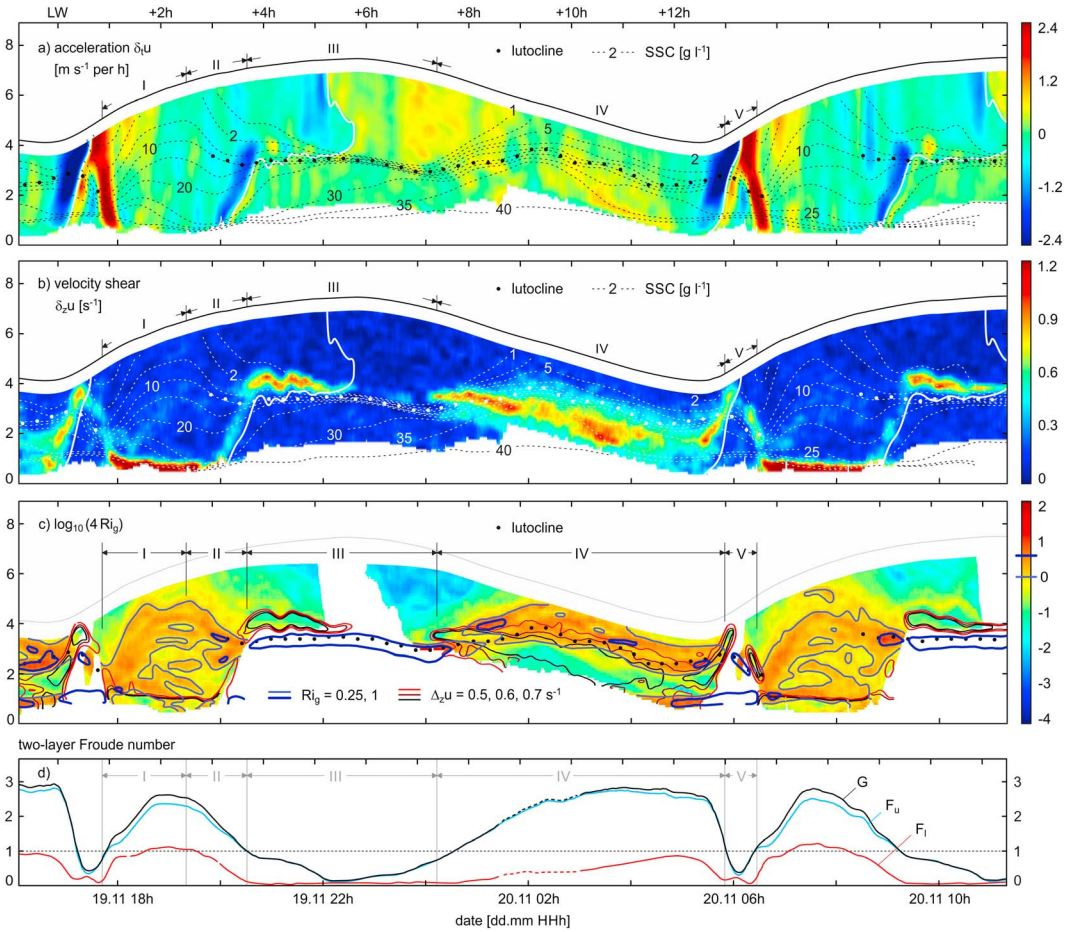

Figure 3. Dynamics and stability. (a) Horizontal velocity acceleration, upstream positive. (b) Vertical velocity shear. (c) Gradient Richardson number, omitting regions of low velocity ($<$ 0.2 m/s). (d) Two-layer Froude number. The boundary between the two layers is defined by the vertical lutocline location or by the 10 g/L isolutal if a local δ_zSSC maximum does not exist.

velocity measured by the upper ECM, showing very low velocities in the fluid mud layer ($<$ 0.15 m/s) layer, up to the increase after 10.5 hr during stage V.

3.3. Restratification and Decoupling

As flood velocities decrease, hindered settling causes increased stratification around the 10 g/L isolutal (Figure 2c, stage II). Subsequently, the water column restratifies. This collapse of the vertical SSC profile is triggered by the positive feedback between stratification and suppression of turbulence, leading to reduced mixing and, again, increased settling (Winterwerp, 2001). At the end of stage II, damping of turbulence by the emerging stratification is indicated by Ri_g reaching maximum values first at the height of the lutocline ($Ri_g > 1$, Figure 3c), which suggests full suppression of turbulence (e.g., Woods, 1969).

After restratification, the upper part of the water column is decoupled from the fluid mud layer. The flow in the fluid mud layer is subsequently ebb directed (maximum 0.15 m/s). Note that the vertical extent of the region of deceleration (lower layer, end of stage II, Figure 3a) aligns with the thickness of the reformed fluid mud layer. In the upper layer, flood-directed flow continues, and salinity increases above the lutocline (Figure 2a, vertical bars). The maximum vertical salinity difference across the lutocline reaches 4 practical salinity units.

4. Discussion

4.1. Restratification and Effects on Advection of Salt

The first part of the flood (stages I and II) is characterized by intense mixing. The shear layer is located near the bed. During restratification the relatively homogenous flow profile develops into a two-layer flow system, and

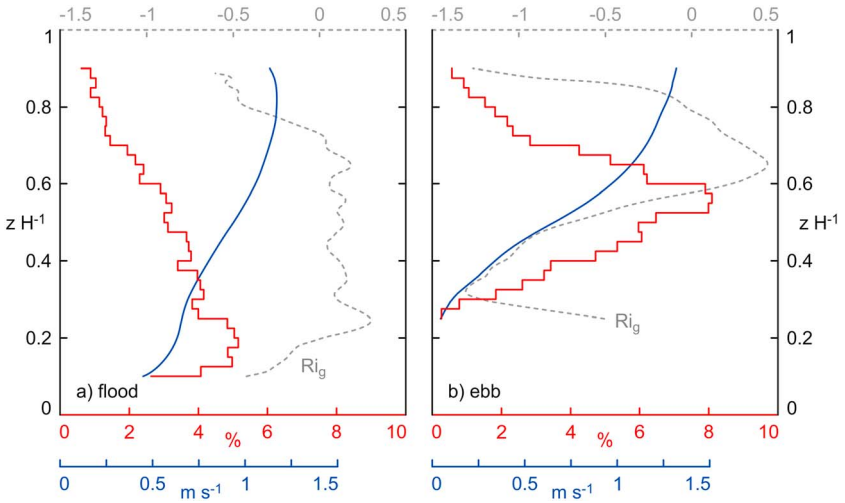

Figure 4. Time-averaged vertical profiles of velocity (blue), sediment transport rate (red), and Ri_g (gray). Averaging periods are (a) stage I (flood) and (b) stage IV (ebb). Velocity and Ri_g are averaged along isolines of relative height ($z\,H^{-1}$). The transport rate is integrated along $z\,H^{-1}$ isolines, and the resulting profile is normalized by the vertical sum.

the shear layer is located above the lutocline. The two-layer view is justified by the composite two-layer Froude number (Figure 4c), which well describes the observed stability of the flow (stages III and V, $G < 1$). The Froude number also indicates the main periods of entrainment (stages I and IV, $G > 1$). During these two stages, the upper layer is always active ($F_u > 1$), while F_l exceeds values of 1 only during stage I, when no distinct stratification exists (Armi & Farmer, 1986).

After restratification the buoyancy frequency reaches peak values of 0.7 s^{-1} at the lutocline (Figure 4b). This exceeds typical values of highly stratified salt wedge estuaries by a factor of 2 (Geyer et al., 2008). Under such conditions, the two layers are dynamically decoupled and stratification effectively prevents downward mixing of momentum. This is clearly the case, as the stratification allows for the development of counterdirected velocities, separated by the lutocline.

The study site is located closer to the downstream end of the fluid mud layer, and the horizontal, sediment-induced pressure gradient is directed downstream. Based on a tidally averaged model, Talke et al. (2009) showed that this pressure gradient is significant, as it reduces the classical estuarine residual flow, near-bed upstream (e.g., Geyer & MacCready, 2014). High water and slack water occur almost at the same time along the respective part of the channel (Winterwerp & Wang, 2013), and the water column is assumed to restratify quasi-simultaneously. The observed collapse of the vertical SSC profile causes a rapid near-surface reduction and near-bed increase of this pressure gradient. It is thus highly probable that the increased pressure gradient controls flow reversal and drives the ebb-directed flow in the lower layer. The restratification must also have an impact on the residual flow profile. The observed flow reversal in the lower layer suggests a reduction of the classical estuarine residual flow. However, the actual contribution of restratification to the residual flow cannot be quantified, based on this data set alone.

The increase of SSC in the fluid mud layer, observed after restratification during stage III, is probably not only due to dewatering but may be supported by inflow of sediments from shallower regions, located toward the banks. It is understood that the contribution of lateral transport to restratification cannot be assessed, since data were collected at a single cross-channel station.

An important consequence of restratification and decoupling is the inverse salinity profile, formed during flood. Lower saline water is trapped in fluid mud at the point in time of restratification, while advection of higher saline water continues in the upper layer. Such inverse salinity profiles were observed also in other high-concentration estuarine domains (e.g., the Huanghe, Wang & Wang, 2010; in the Gironde, Sottolichio et al., 2011; or in the Ouse estuary, Uncles et al., 2006). Here the hydraulic cross section is reduced due to mud-induced stratification, which increases the salinity intrusion in the upper layer, into the estuary. In general, the occurrence of inverse salinity profiles demonstrates the main attribute of hyperturbid systems, that is, that density structure and flow patterns are controlled by SSC, not by salinity.

4.2. Transport and Entrainment

Mud transport during flood (stage I) is restricted to the period between entrainment and restratification, since transport declines with the reformation of the fluid mud layer (Figure 2d). Importantly, the flood transport period is considerably shorter than the overall flood duration, due to the early restratification. Despite rapid entrainment and increase of SSC in the upper water column, most of the flood transport occurs closer to the bed (Figure 4a), due to the relatively homogenous velocity profile. The flow is then supercritical (Figure 3d, stages I and II), which confirms the analyses of Winterwerp et al. (2017) for flood transport.

Regarding the ebb phase (stage IV), the same study suggested fluid mud to slowly migrate downstream (as a whole). While the lower part of the fluid mud layer indeed migrates with a very low velocity, results here indicate that the situation is more complex. The part of the profile where active mixing occurs ($Ri_g < 0.25$, Figure 3c, stage IV) resembles an interfacial mixing zone, as it is found to develop in strongly stratified systems, for example, at the top of an eroding salt wedge (e.g., Geyer et al., 2010).

The zone is located between the nonturbulent, lower part of the fluid mud layer and the stratified upper part of the water column ($N \cong 0.4\ s^{-1}$). The upper part is characterized by high Ri_g (≥ 1, Figure 3c, stage IV), which indicates self-stratifying behavior of the suspension, as entrained sediments induce stratification and dampen further upward mixing (Geyer & Smith, 1987; Middleton, 1993). At the same time, the stratification prevents downward mixing of momentum. Fluid mud closer to the bed therefore remains stationary until the region of maximum shear approaches the bed before ebb slack water.

Consequently, most of the ebb-directed sediment transport is confined to a shallow region in the center of the water column (Figure 4b), and no transport occurs close to the bed. This situation is understood as a specific case of shear dispersion, which likely explains the (observed) reduction in layer thickness and also the increase of its along-channel extent after the ebb phase, as shown by Talke et al. (2009, their Figures 4 and 5).

Fluid mud layer thickness and its overall structure are considered to adjust continuously to changes in hydrodynamic conditions. Measured ebb velocities (which exceed flood velocities, Figure 2a) might suggest that here an adjustment is observed, in response to the slight increase in discharge (Figure 1c), potentially leading to a downstream displacement of the fluid mud layer. However, the discharge is still moderate (Winterwerp et al., 2017), and the observed layer thickness aligns with observations of Talke et al. (2009). So far, the observed aspects of fluid mud transport, entrainment, and restratification are assumed to be phenomenologically representative for equilibrium conditions in the Ems estuary, that is, a constant fluid mud layer structure, when averaged over several tidal cycles.

To maintain this dynamic equilibrium in fluid mud layer structure, upstream pumping of mud during flood must be balanced by the observed shear dispersion during ebb (transport profiles, Figure 4). It should be emphasized that this balance is conceptually similar to estuarine sediment transport as observed in presence of (classical) tidal straining (Becherer et al., 2016; Jay & Musiak, 1994), where differential advection of a horizontal salinity gradient leads to periodic density stratification (Simpson et al., 1990). The major difference is that here in a hyperturbid tidal channel, density stratification depends on SSC and on the response of internal processes, for example, hindered settling and entrainment, to asymmetric tidal forcing. It follows for hyperturbid conditions that intratidal variations in velocity shear and mud transport are controlled by the feedback of mud-induced periodic stratification on the flow, as shown in this study by an analysis of the entrainment asymmetry and rapid restratification, which occurs early during flood.

5. Summary and Conclusions

Observations in a hyperturbid estuarine channel demonstrate the effect of mud-induced periodic stratification on flow and transport of mud. The water column exhibits a two-layer structure, except for the first part of the flood phase, when mud-induced stratification is eroded by quasi-instantaneous entrainment and vertical mixing. The flood transport period is considerably shorter than the overall flood duration. It is delimited by rapid settling of sediment, which restores the two-layer structure. Then, lower saline water is trapped in fluid mud, and the hydraulic cross section is reduced, which increases the salinity intrusion into the estuary at the end of flood, leading to the development of an inverse salinity profile. Entrainment during ebb occurs only at the fluid mud layer surface. Layer thickness is gradually reduced, while fluid mud is almost stationary near the bed. In case of a dynamic equilibrium of fluid mud layer location and thickness, pumping of mud during

flood must be balanced by shear dispersion during ebb. These results, showing details of the relation between velocity shear, entrainment, and transport, are anticipated to facilitate more realistic modeling scenarios and to eventually allow for better predictions of the dynamic behavior of fluid mud in hyperturbid estuarine channels.

Acknowledgments
This study was funded through DFG-Research Center/Cluster of Excellence "The Ocean in the Earth System." Marius Becker is funded by the German Federal Waterways Engineering and Research Institute (BAW). The Senckenberg Institute is thanked for providing the ship time. The authors gratefully acknowledge the help of Eva Kwoll, Gabriel Herbst, and Knut Krämer during data collection. The data are available through the PANGAEA data base (https://doi.pangaea.de/10.1594/PANGAEA.890517).

References

Armi, L., & Farmer, D. (1986). Maximal two-layer exchange flow through a contraction with barotropic net flow. *Journal of Fluid Mechanics*, *64*, 27–51.

Becherer, J., Flöser, G., Umlauf, L., & Burchard, H. (2016). Estuarine circulation versus tidal pumping: Sediment transport in a well-mixed tidal inlet. *Journal of Geophysical Research: Oceans*, *121*, 6251–6270. https://doi.org/10.1002/2016JC011640

Bruens, A., Winterwerp, J., & Kranenburg, C. (2012). Physical and numerical modeling of the entrainment by a high-concentration mud suspension. *Journal of Hydraulic Engineering*, *138*(6), 479–490. https://doi.org/10.1061/(ASCE)HY.1943-7900.0000545

Cao, Z., Wang, X. H., Guan, W., Hamilton, L. J., Chen, Q., & Zhu, D. (2012). Observations of Nepheloid layers in the Yangtze estuary, China, through phase-corrupted acoustic Doppler current profiler speeds. *Marine Technology Society Journal*, *46*(4), 60–70. https://doi.org/10.4031/MTSJ.46.4.6

Chernetsky, A., Schuttelaars, H., & Talke, S. (2010). The effect of tidal asymmetry and temporal settling lag on sediment trapping in tidal estuaries. *Ocean Dynamics*, *60*(5), 1219–1241. https://doi.org/10.1007/s10236-010-0329-8

De Jonge, V. N., Schuttelaars, H. M., van Beusekom, J. E. E., Talke, S. A., & de Swart, H. E. (2014). The influence of channel deepening on estuarine turbidity levels and dynamics, as exemplified by the Ems estuary. *Estuarine, Coastal and Shelf Science*, *139*, 46–59. https://doi.org/10.1016/j.ecss.2013.12.030

Dijkstra, Y. M., Schuttelaars, H. M., & Winterwerp, J. C. (2018). The hyperturbid state of the water column in estuaries and rivers: The importance of hindered settling. *Ocean Dynamics*, *68*(3), 377–389. https://doi.org/10.1007/s10236-018-1132-1

Donker, J. J. A., & Swart, H. E. (2013). Effects of bottom slope, flocculation and hindered settling on the coupled dynamics of currents and suspended sediment in highly turbid estuaries, a simple model. *Ocean Dynamics*, *63*(4), 311–327. https://doi.org/10.1007/s10236-013-0593-5

Geyer, W. R., Hill, P. S., & Kineke, G. C. (2004). The transport, transformation and dispersal of sediment by buoyant coastal flows. *Continental Shelf Research*, *24*(7–8), 927–949.

Geyer, W. R., Lavery, A. C., Scully, M. E., & Trowbridge, J. H. (2010). Mixing by shear instability at high Reynolds number. *Geophysical Research Letters*, *374*, L22607. https://doi.org/10.1029/2010GL045272

Geyer, W. R., & MacCready, P. (2014). The estuarine circulation. *Annual Review of Fluid Mechanics*, *46*(1), 175–197. https://doi.org/10.1146/annurev-fluid-010313-141302

Geyer, W. R., Scully, M., & Ralston, D. (2008). Quantifying vertical mixing in estuaries. *Environmental Fluid Mechanics*, *8*(5-6), 495–509. https://doi.org/10.1007/s10652-008-9107-2

Geyer, W. R., & Smith, J. D. (1987). Shear instability in a highly stratified estuary. *Journal of Physical Oceanography*, *17*(10), 1668–1679. https://doi.org/10.1175/1520-0485(1987)017%3C1668:SIIAHS%3E2.0.CO;2

Jay, D. A., & Musiak, J. D. (1994). Particle trapping in estuarine tidal flows. *Journal of Geophysical Research*, *99*, 20,445–20,461. https://doi.org/10.1029/94JC00971

Kineke, G. C., Sternberg, R. W., Trowbridge, J. H., & Geyer, W. R. (1996). Fluid mud processes on the Amazon continental shelf. *Continental Shelf Research*, *16*(5–6), 667–696. https://doi.org/10.1016/0278-4343(95)00050-X

Kirby, R., & Parker, W. R. (1983). Distribution and behavior of fine sediment in the Severn Estuary and Inner Bristol Channel, U.K. *Canadian Journal of Fisheries and Aquatic Sciences*, *40*, 83–95.

Middleton, G. V. (1993). Sediment deposition from turbidity currents. *Annual Review of Earth and Planetary Sciences*, *21*(1), 89–114. https://doi.org/10.1146/annurev.ea.21.050193.000513

Richardson, L. F. (1920). The supply of energy from and to atmospheric eddies. *Proceedings of the Royal Society of London, Series A*, *97*(686), 354–373. https://doi.org/10.1098/rspa.1920.0039

Simpson, J., Brown, J., Matthews, J., & Allen, G. (1990). Tidal straining, density currents, and stirring in the control of estuarine stratification. *Estuaries and Coasts*, *13*(2), 125–132. https://doi.org/10.2307/1351581

Sottolichio, A., Hurther, D., Gratiot, N., & Bretel, P. (2011). Acoustic turbulence measurements of near-bed suspended sediment dynamics in highly turbid waters of a macrotidal estuary. *Continental Shelf Research*, *31*(10), S36–S49.

Talke, S. A., de Swart, H. E., & Schuttelaars, H. M. (2009). Feedback between residual circulations and sediment distribution in highly turbid estuaries: An analytical model. *Continental Shelf Research*, *29*(1), 119–135. https://doi.org/10.1016/j.csr.2007.09.002

Talke, S. A., Swart, H. E., & Jonge, V. N. (2011). An idealized model and systematic process study of oxygen depletion in highly turbid estuaries. *Estuaries and Coasts*, *32*(4), 602–620.

Trowbridge, J. H., & Kineke, G. C. (1994). Structure and dynamics of fluid muds on the Amazon continental shelf. *Journal of Geophysical Research*, *99*, 865–874. https://doi.org/10.1029/93JC02860

Uncles, R. J., Stephens, J. A., & Law, D. J. (2006). Turbidity maximum in the macrotidal, highly turbid Humber Estuary, UK: Flocs, fluid mud, stationary suspensions and tidal bores. *Estuarine, Coastal and Shelf Science*, *67*(1–2), 30–52. https://doi.org/10.1016/j.ecss.2005.10.013

Van Maren, D. S., Winterwerp, J. C., & Vroom, J. (2015). Fine sediment transport into the hyper-turbid lower Ems River: The role of channel deepening and sediment-induced drag reduction. *Ocean Dynamics*, *65*(4), 589–605. https://doi.org/10.1007/s10236-015-0821-2

Wang, X., & Wang, H. (2010). Tidal straining effect on the suspended sediment transport in the Huanghe (Yellow River) Estuary, China. *Ocean Dynamics*, *60*(5), 1273–1283. https://doi.org/10.1007/s10236-010-0298-y

Winterwerp, J. C. (2001). Stratification effects by cohesive and non-cohesive sediment. *Journal of Geophysical Research*, *106*, 22,559–22,574. https://doi.org/10.1029/2000JC000435

Winterwerp, J. C. (2002). On the flocculation and settling velocity of estuarine mud. *Continental Shelf Research*, *22*(9), 1339–1360. https://doi.org/10.1016/S0278-4343(02)00010-9

Winterwerp, J. C. (2011). Fine sediment transport by tidal asymmetry in the high-concentrated Ems River: indications for a regime shift in response to channel deepening. *Ocean Dynamics*, *61*(2–3), 203–215.

Winterwerp, J. C., Vroom, J., Wang, Z.-B., Krebs, M., Hendriks, E. C. M., van Maren, D. S., et al. (2017). SPM response to tide and river flow in the hyper-turbid Ems River. *Ocean Dynamics*, *67*(5), 559–583. https://doi.org/10.1007/s10236-017-1043-6

Winterwerp, J. C., & Wang, Z. B. (2013). Man-induced regime shifts in small estuaries—I: Theory. *Ocean Dynamics*, *63*(11–12), 1279–1292. https://doi.org/10.1007/s10236-013-0662-9

Wolanski, E., Chappell, J., Ridd, P., & Vertessy, R. (1988). Fluidization of mud in estuaries. *Journal of Geophysical Research*, *93*, 2351–2361. https://doi.org/10.1029/JC093iC03p02351

Woods, J. D. (1969). On Richardson's Number as a Criterion for Laminar-Turbulent-Laminar Transition in the Ocean and Atmosphere. *Radio Science*, *4*(2), 1289–1298.